

TOP MASS MEASUREMENTS AT THE TEVATRON RUN II

Gueorgui V. Velev

e-mail: velev@fnal.gov

*Fermi National Accelerator Laboratory, Batavia, IL 60510**for**the CDF and DØ collaborations***Abstract**

The latest top quark mass measurements by the CDF and DØ experiments are presented here. The mass has been determined in the dilepton ($t\bar{t} \rightarrow e\mu, ee, \mu\mu + \text{jets} + \cancel{E}_T$) and lepton plus jets ($t\bar{t} \rightarrow e \text{ or } \mu + \text{jets} + \cancel{E}_T$) final states. The most accurate single result from lepton plus jets channel is $173.5^{+3.7}_{-3.6}(\text{stat.} + \text{Jet Energy Scale Systematic}) \pm 1.3(\text{syst.})$ GeV/c², which is better than the combined CDF and DØ Run I average. A preliminary and unofficial average of the best experimental Run II results gives $M_{top} = 172.7 \pm 3.5$ GeV/c².

1 Introduction

Since the first evidence in 1994 ¹⁾ and the discovery of the top quark in 1995 ^{2) 3)}, the CDF and DØ Collaborations invested a lot of work to determine its properties, specially the value of its mass, which is a fundamental parameter of the Standard Model (SM). The ongoing Run II, with the upgraded Fermilab Tevatron collider and CDF and DØ detectors, gives new possibilities for a precise measurement of the top mass. Due to its large mass, corresponding to a Yukawa coupling of order unity, one may suspect that the top quark may have a special role in the electroweak symmetry breaking. In addition, due to its significant contribution to high order radiative corrections of a number of electroweak observables, a precise measurement of the top quark mass provides a tighter constrain on the Higgs mass ⁴⁾.

This paper reports on the latest CDF and DØ top quark mass results which are based on about 318 pb⁻¹ (CDF) and 219 pb⁻¹ (DØ) of data from the first two years of the Tevatron Run II (2002 to 2004). Another paper, presented on this conference ⁵⁾, summarized the top quark kinematics properties including its recently measured production cross section at the center of mass energy of $\sqrt{s}=1.96$ TeV,

At this Tevatron energy, top quarks are produced generally in pairs from the processes $q\bar{q} \rightarrow t\bar{t}$ (in $\sim 85\%$ of the cases) and $gg \rightarrow t\bar{t}$ (in $\sim 15\%$ of the cases). Top can be produced as a single quark by electroweak interactions, by W-gluon fusion or virtual W* production in the s-channel ⁶⁾, but with a smaller cross section. At this time, no signal has been observed from single top processes and they are not expected to be utilized for a precise mass measurement.

In the Standard Model the branching ratio of the decay $t \rightarrow bW$ is nearly 100%. When a $t\bar{t}$ pair is produced, each of the W-bosons can decay into either a charged lepton and a neutrino (branching ratio of 1/9 for each lepton family) or into a $q\bar{q}'$ quark pair (branching ratio of 2/3). This allows us to classify the final states as:

- Dilepton final state, when both W's from the $t\bar{t}$ pair decay leptonically. This state is characterized by two high P_T charged leptons, two jets from $b\bar{b}$ quarks ¹ and significant missing transverse energy (E_T) from the neutrinos.
- Lepton plus jets final state, when one W boson decays leptonically and the other one hadronically. This state contains one high P_T charged

¹Errors in jet reconstruction and gluon radiation in the event may make the observed number of jets smaller or larger. This statement is valid for all final states.

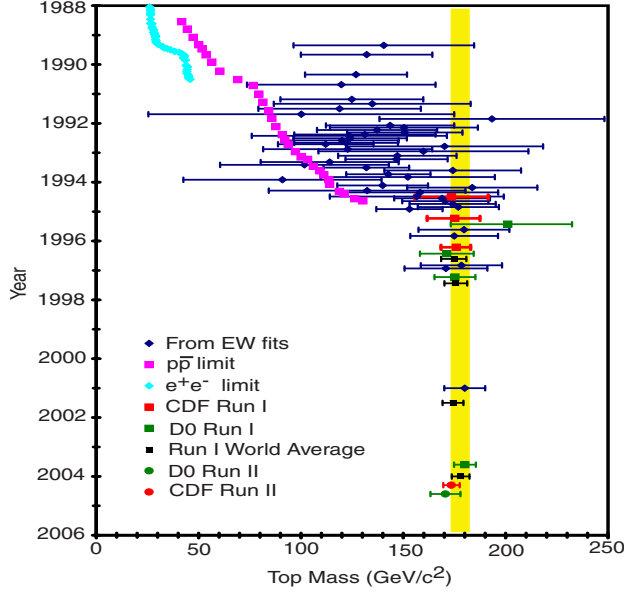


Figure 1: *The summary of the top mass “evaluations” and direct measurements versus time. See the text for explanation of the points.*

lepton, four jets and significant \cancel{E}_T .

- All hadronic final state, when both W’s decay hadronically. This state is characterized by 8 jets, two of which are from b -quarks.

In Run I, CDF and DØ used all of these signatures for the top mass measurements. At this time, the Run II top mass analyses from the all-hadronic channel are still in progress and will not be reported in this paper.

Figure 1 shows how our knowledge on the top quark mass improved with time. The diamonds represent the indirect determinations from fits to the electroweak observables ⁷⁾. The curves in the upper left corner of the figure represent the limits from direct searches in e^+e^- and $p\bar{p}$ machines. The Run I CDF and DØ results are presented with squares. The filled circles are the new Tevatron Run II results. The band represents the average Run I top mass results. One observes that the recent Tevatron results have equal or better accuracy than the Run I world average.

2 Top kinematics and mass reconstruction methods

The kinematics of the events in the lepton plus jets final state is over-constrained. In this channel, the number of measured quantities and the number of applicable energy-conservation equations, from five production and decay vertices, are larger than the number of non-measured kinematical event parameters. This feature allows for a complete reconstruction of the four-momenta of the final state particles in the event, for example using the two constrain kinematical fit (2CF), and for a reconstruction of the top mass event-by-event. In this type of analysis there is an ambiguity in how to assign the four leading jets to the two b quarks and two light quarks coming from the $t\bar{t}$ system. If none of these jets is tagged by b taggers ², there are 12 different ways of assigning jets to the 4 partons. Combining with the ambiguity from solving of a quadratic equation on P_z^ν , there are 24 different values of m_{top} returned by the fit. The combinations are reduced to 12 or to 4 if one or two of the jets are selected from b -taggers.

The variety of the CDF and DØ analyses in the lepton plus jet sample is relatively large. However, all analyses can be separated in three major categories:

1. Template type analyses, where the reconstructed mass distribution from the data is compared with expected distributions from Monte Carlo generated signal (mass-dependent) and background. In these types of analyses, all events are weighted equally. By doing so one neglects the additional information coming from a different mass resolution in single events. In addition no use is made of possible information from the dynamic of the process which can be assumed to be known. Typical examples for this type of analysis are the CDF and DØ Run I ¹⁰⁾ ¹¹⁾ and the latest, most accurate CDF Run II lepton plus jets analysis, described in Section 3.1.
2. Matrix Element type analyses, originally proposed by Dalitz and Goldstein ¹²⁾ and independently by Kondo ¹³⁾. These methods calculate the posterior probability, given the known production cross section, for every event with measured kinematic properties, to originate from a $p\bar{p} \rightarrow t\bar{t}$ process. A typical example is the DØ Matrix Element analysis which is the base of the best Run I top mass measurement ¹⁴⁾. In Run II CDF uses a method, proposed by K.Kondo ¹³⁾, called Dynamic Likelihood Analysis, which differs in the way that the normalization of the differential cross section is performed.

²CDF and DØ use taggers based on either displaced vertices (Secondary Vertex Tagging, SVX, for example see ⁸⁾) or on low P_T electrons or muons from the b -quark semileptonic decays (Soft Lepton Tagging, SLT ⁹⁾)

3. A mixture between methods 1) and 2). For example the $t\bar{t}$ event is reconstructed using the kinematic algorithms similar to the template analyses but an event-by-event probability of each kinematic reconstruction is exploited as a weight (for example $\exp(-\frac{\chi^2}{2})$). A typical example of this category is the DØ Ideogram Analysis ¹⁵⁾.

3 Lepton plus jet channel

3.1 CDF result

For the time being the most accurate top quark mass measurement comes from the lepton plus jets channel. This channel combines the benefits of good signal to background ratio, the possibility to reconstruct the top quark mass event by event with a relatively small combinatorial effect, and a large branching fraction. In brief, we discuss below the main selection criteria for this channel.

Lepton plus jets events have the signature $p\bar{p} \rightarrow t\bar{t}X \rightarrow \ell\nu b q\bar{q}'\bar{b}X$. The characteristics of this final state begins with the identification of one isolated central high energy lepton (e with $E_T > 20$ GeV or μ with $P_T > 20$ GeV) and $|\eta| < 1$ ³.

Assuming that the lepton is coming from W boson decay, a companion neutrino should exist. This would spoil the balance of the observed momentum in the transverse plane. The missing transverse energy (\cancel{E}_T) is constructed by adding the calorimeter energy vectors in the plane transverse to the beam. The calorimeter clusters identified as jets are corrected for detector response and for multiple $p\bar{p}$ interactions. In muon events the \cancel{E}_T is computed using the muon momentum measured by the track instead of the muon calorimeter signal.

In order to fully reconstruct the $t\bar{t}$ system, at least four central jets $|\eta| \leq 2$ are required in the system. The SVX tagging algorithm is run over the leading jets ($E_T > 15$ GeV): some of them may be identified as b-jets. To obtain maximum statistical benefit from the event sample it is helpful to decompose it into several classes of events which are expected to have different signal-to-background ratios and top mass resolutions. The Monte Carlo studies showed that an optimal partitioning is obtained splitting the sample into four statistically independent categories: events with double SVX tags (2SVX), events with single SVX tag and tight forth jet cut (four jets with $E_T > 15$ GeV, 1SXVT), events with single SVX tag and loose forth jet cut ($15 > E_T > 8$ GeV for the 4th jet, 1SXVL) and finally events without tags (0-tag). Since the last sample has a high background contamination compared to SVX tagged ones, an additional

³A complete description of the lepton selection, including all cuts used, can be found elsewhere ¹⁶⁾

Table 1: *In the first four columns from left to right: lepton plus jets subsamples used in the top quark mass analysis, number of events in each sample, S/B ratio, and a summary of the jet energy cut selection are presented. A total of 165 $t\bar{t}$ candidates were selected. The last column summarizes the background fractions in % from $W + \text{light quark}$, $Wb\bar{b} + Wc\bar{c} + Wc$ and QCD multijet events (left to right).*

Data Subsample	Number of events	S/B	Jet E_T cuts (GeV) jets 1-3 (4^{th} jet)	Bckg. type and fraction in %
2SVX	25	10.6/1	$E_T > 15$ ($E_T > 15$)	21/59/10
1SVXT	63	3.7/1	$E_T > 15$ ($E_T > 15$)	17/38/22
1SVXL	33	1.1/1	$E_T > 15$ ($15 > E_T > 8$)	29/48/14
0-tag	44	0.9/1	$E_T > 21$ ($E_T > 21$)	75/3/20

optimization of the jet E_T cuts ($E_T > 21$ GeV) was performed. A total of 165 $t\bar{t}$ candidates were selected from 318 pb^{-1} of data.

The dominant backgrounds in all samples are direct W plus multijet production, including heavy flavour production, and QCD multijet events where one jet is misidentified as a lepton. Additional small backgrounds are due to WW/WZ and single top production. The amount and composition of the background depends on the sample. In the case of the 2SVX sample, the $Wb\bar{b} + Wc\bar{c} + Wc$ background dominates ($\sim 60\%$) while in the case of the 0-tag sample, the W plus light quark production is responsible for $\sim 75\%$ of background. The information for these four subsamples, including the dominant type and background fraction, is summarized in Table 1.

Each event, either from data or MC samples, is fitted to the hypothesis $t\bar{t}X \rightarrow \ell\nu b q \bar{q}' \bar{b}X$. We use four kinematic constraints, as a consequence of the assumed lepton plus jets event structure ($M_{\ell\nu} = M_{jj} = M_W$ and $M_{\ell\nu b} = M_{jjb} = M_{\text{top}}$). The fitting procedure runs over all possible 24 combinations of assigning the four leading jets to the b , \bar{b} and $W \rightarrow q\bar{q}'$ partons (the order of the pair assigned to the W is irrelevant). If one or two of the four leading jets are tagged as a b -jets, they are assigned to the b -partons and the number of explored combinations is correspondingly smaller. All solutions with $\chi^2 < 9$ (cut optimized on the MC studies) are accepted. The top mass value corresponding to the combination with the minimum χ^2 is picked as the mass value indicated by the event.

The events from the MC samples are used to produce probability density distributions or so-called templates. In case of the signal MC, these distributions are parameterized as a function of reconstructed and input top masses. On the other hand, the background probability density distributions are parameterized only as a function of the reconstructed mass. The likelihood of

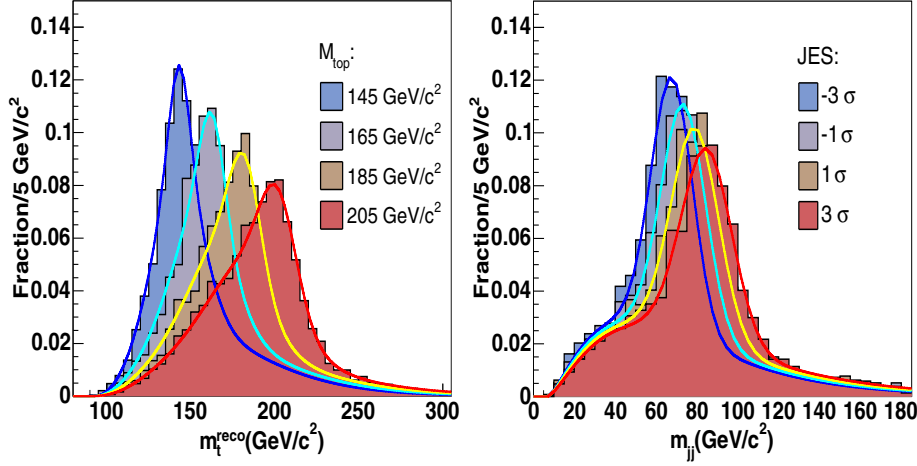


Figure 2: *Left: reconstructed top mass p.d.fs for input top masses from 145 to 205 GeV/c^2 and $\text{JES} = 0$. Right: reconstructed mass p.d.fs of the dijet system attributed to the W for different JES values in the range of -3σ – $+3\sigma$ and input top mass of 180 GeV/c^2 .*

each subsample uses the parameterized signal and background probability density functions (p.d.f) to evaluate the dependence of the likelihood on the input top mass.

To reduce the dominant systematic error coming from jet energy scale (JES) ¹⁰⁾ the latest CDF template analysis exploits the fact that the global JES scale can be determined from the decay $W \rightarrow q\bar{q}'$. MC studies have shown that this technique provides a 22% reduction in the JES uncertainty. Similar template distributions as for the kinematically reconstructed top mass are built for the dijet mass, with the exceptions of removing the $\chi^2 < 9$ requirement, exploiting all the possible jet-to-parton assignments in the event. Examples of top and dijet reconstructed masses p.d.fs are shown on Figure 2 left and right respectively.

The reconstructed top and W dijet mass values for every data event are simultaneously compared to the p.d.fs from signal and background sources

Table 2: *The systematic uncertainties in the CDF lepton plus jets top quark mass measurement.*

Source	ΔM_{top} (GeV/ c^2)
b-jets modeling	0.6
Method	0.5
Initial state radiation	0.4
Final state radiation	0.6
Shape of background spectrum	0.8
b -tag bias	0.1
Parton distribution functions	0.3
Monte Carlo generators	0.2
MC statistics	0.3
Total	1.5

performing an unbinned likelihood fit. The fit finds a maximum likelihood value according to: the expected numbers of signal and background events in each subsample, the JES and the true top quark mass (M_{top}). Only M_{top} is a free parameter in the likelihood fit, the other are constrained within their uncertainties. For each subsample, the likelihood has the following form:

$$\mathcal{L} = \mathcal{L}_{shape}^{M_{top}} \cdot \mathcal{L}_{shape}^{m_{jj}} \cdot \mathcal{L}_{counting} \cdot \mathcal{L}_{bg}. \quad (1)$$

In (1), the main information on the top quark mass is hidden in the term $\mathcal{L}_{shape}^{M_{top}}$. It gives the probability for an event with reconstructed top mass m_{top}^{rec} to come from true top mass M_{top} . All other terms constrain the JES ($\mathcal{L}_{shape}^{m_{jj}}$), the number of observed events ($\mathcal{L}_{counting}$) and number of expected backgrounds in the subsample (\mathcal{L}_{bg}) and help to reduce the statistical and systematical uncertainties returned by the fit.

The systematic uncertainties are summarized in Table 2. For each systematic source, the relevant parameters are varied by $\pm 1\sigma$ in the $t\bar{t}$ MC sample with $M_{top}=178$ GeV/ c^2 and sets of fake events are generated. These fake events are reconstructed in the same way as normal events. This procedure is called “pseudoexperiments” (PE). It propagates the $\pm 1\sigma$ effects to a shift in the top mass relative to the result from the nominal sample.

The reconstructed top masses in the four subsamples with overlaid best fit for the signal and background MC expectation are shown in Figure 3. The combined fit for all lepton plus jets events returned $M_{top} = 173.5_{-3.6}^{+3.7}(\text{stat.}+\text{JES}) \pm 1.3(\text{syst.})$ GeV/ c^2 and $\text{JES} = -0.10_{-0.91}^{+0.89}(\text{stat.}+\text{syst.})$. This is the most precise single measurement available to date, better than the average Run I result.

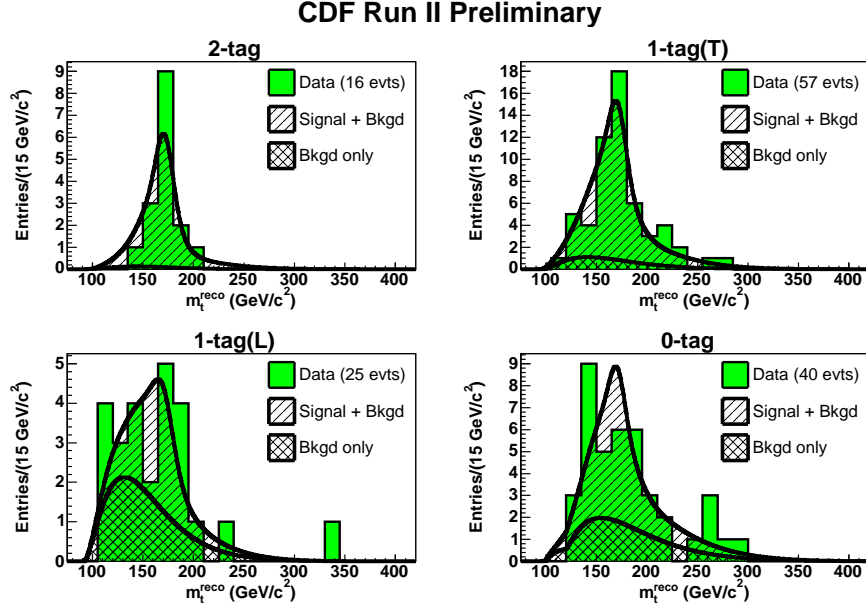


Figure 3: The reconstructed mass distribution (histogram) for each lepton plus jets CDF subsamples is overlaid with the result of the likelihood fit (signal+background, hatched area). The cross hatched area represents only the background.

3.2 $D\bar{O}$ Result

$D\bar{O}$ has measured the top quark mass in the lepton plus jets channel as well. The utilized data set corresponds to an integrated luminosity of approximately 229 pb^{-1} collected between April 2002 and March 2004.

The event selection criteria are similar to those used in CDF. As a first selection step, an identification of the a high P_T isolated electron or muon accompanied by substantial large $\cancel{E}_T > 20 \text{ GeV}$ is required. The isolated electron (muon) candidate should have $P_T > 20 \text{ GeV}$, satisfy a pseudo-rapidity cut of $|\eta| < 1.1$ ($|\eta| < 2.0$) and tight quality conditions. These initial selections provide the data sample.

Two separated analyses, b-tagged and topological, are performed on this sample. In the b-tagged analysis, to reconstruct the top mass the events are additionally selected to have at least 4 jets with $P_T > 15 \text{ GeV}$ and $|\eta| < 2.5$. A

further requirement of identification of one or more jets as b -jets is made. A jet is b -tagged based on the reconstruction of the secondary vertices using the charged particle tracks associated with it. 49 (29) e +jets (μ + jets) b -tagged events survive all cuts and are kinematically fitted to the $t\bar{t}$ hypothesis. In 42 (27) electron (muon) events the kinematic fit converged in a configuration where the lowest χ^2 solution is consistent with b -tagged jet permutation.

In the second analysis the information of the b -tagger is not exploited. To increase the signal to background ratio several modifications of the selection cuts are applied. For example the transverse momenta of the first four jets are increased to 20 GeV. There are 87 e +jets and 80 μ +jets events left after this requirement. Next, using the specific kinematics of the $t\bar{t}$ events, a discriminant (D) was constructed. It is designed to use variables which are uncorrelated or minimally correlated with the top quark mass ¹¹). Four topological variables are considered:

- \cancel{E}_T - missing transverse energy which comes from the neutrino of the W leptonic decay.
- \mathcal{A} - aplanarity of the event. It exploits the fact that the decay products from a massive particle have large aplanarity.
- H'_{T2} - the ratio of the scalar sum of the P_T of the jets, excluding the leading jet, and the scalar sum of $|p_z|$ of the jets, the lepton and of the reconstructed neutrino.
- K'_{Tmin} - a measure of the jet separation folded with the E_T of the reconstructed leptonic W boson.

Figure 4 shows the simulated discriminant distribution for signal and background. A cut of $D > 0.4$ is imposed to select the signal rich region. After the kinematical fit at least one jet permutation is required to have $\chi^2 < 10$.

Similar to the CDF lepton plus jets analysis, two dominant sources of background are accounted for: W plus multijet production, including heavy flavour, and QCD multijet events where one of the jets is misidentified as a lepton and there is significant \cancel{E}_T imbalance in the event due to detector resolution.

The systematic uncertainties of both analyses are summarized in Table 3. The main contributions are due to JES, gluon radiation (initial state-ISR and final state-FSR), and the MC $t\bar{t}$ signal modeling.

As expected, the dominant systematic uncertainty originates from the JES. The impact of JES on the reconstructed top mass was evaluated by scaling the jet energies by $\pm 1\sigma$ for both signal and background in the MC simulation. The uncertainty on the JES was conservatively assumed to be 5% for the $E_T^{jet} >$

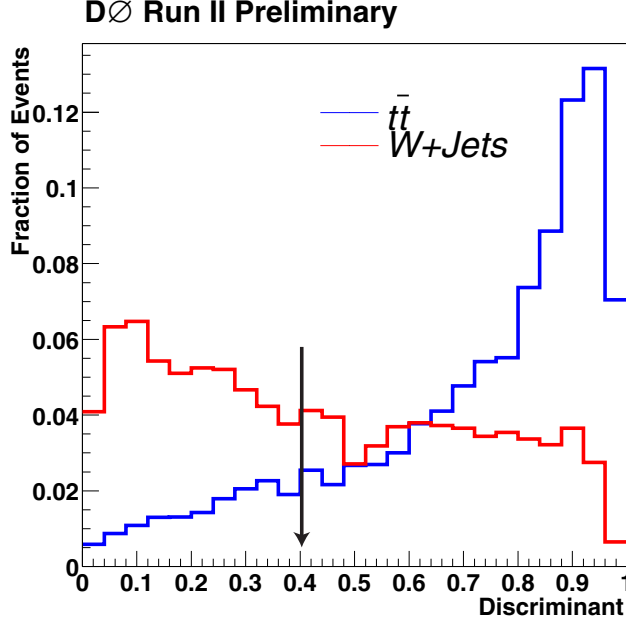


Figure 4: *Discriminant D for $t\bar{t}$ (solid dark line) and background (solid light line) events from MC simulation.*

30 GeV. For jets with $E_T^{jet} < 30$ GeV, the JES uncertainty decreases linearly as $\sigma = 30\% - 25\% \times (E_T^{jet}/30)$ GeV.

Next in importance to the JES is the systematic uncertainty coming from gluon radiation. Regardless of which jet permutation is used, the fitted mass will not be correct if the a radiated gluon is one in the four leading jets in the event. To understand how this affects the $t\bar{t}$ reconstruction, MC events with only four partons hadronizing and forming four jets were compared to events where one of the leading 4 jets comes from gluon radiation. A small deviation of ~ 0.2 GeV/ c^2 from the nominal top mass is observed when the events without gluon radiation are reconstructed. The difference becomes ~ 2.4 GeV/ c^2 when one of the leading jets is a radiated gluon.

In this analyses the model of the kinematic properties of the events is taken directly from MC simulation. Therefore some deficiencies in the MC model may lead to a substantial bias in the mass reconstruction. In order to perform a conservative estimate of this possible effect, in addition to the nominal sample for $t\bar{t}$ signal a complementary sample was generated where an

Table 3: Systematic uncertainties in the $D\bar{O}$ lepton plus jets top quark mass measurement. The uncertainty on JES, Gluon Radiation and Signal Model are the dominant sources of error on the mass.

Source	ΔM_{top} (GeV/c ²)	
	b-tagged analysis	Topological Analysis
JES	+4.7/-5.3	+6.86.5
Jet Resolution	± 0.9	± 0.9
Gluon Radiation	± 2.4	± 2.6
Signal Model	+2.3	+2.3
Background Model	± 0.8	± 0.7
b -tagging	± 0.7	N/A
Calibration	± 0.5	± 0.5
Trigger bias	± 0.5	± 0.5
MC statistics	± 0.5	± 0.5
Total	± 6.0	+7.8-7.1

additional parton is produced in association with the $t\bar{t}$ pair. The cross section for this process is approximately two times smaller than the cross section for the $t\bar{t}$ production. By analyzing this sample, an uncertainty of +2.3 GeV/c² due to the uncertainty on signal modeling is assigned to the analyses. All other possible systematic effects turned out to be relatively small, at the level of 0.5~0.7 GeV/c².

The distributions of the fitted masses and $-\ln(\mathcal{L})$ curves are shown in Figure 5. The top two figures show the result from the b -tagged analysis while the bottom two represent the topological one. Taking into account the output from the binned likelihood fit and the systematic uncertainties the final result for the analyses is $M_{top} = 170.6 \pm 4.2(\text{stat.}) \pm 6.0(\text{syst.})$ GeV/c² (b -tagged analysis) and $M_{top} = 169.9 \pm 5.8(\text{stat.})^{+7.8}_{-7.1}(\text{syst.})$ GeV/c² for the topological one.

4 Dilepton Channel

4.1 CDF result

CDF has several independent dilepton analyses which are found to return consistent values for the top mass. Since this sample has good signal to background ratio ($\sim 4/1$) one is stimulated to invent ingenious ways to reconstruct the events and extract M_{top} .

The event selection criteria are similar as in the lepton plus jets channel.

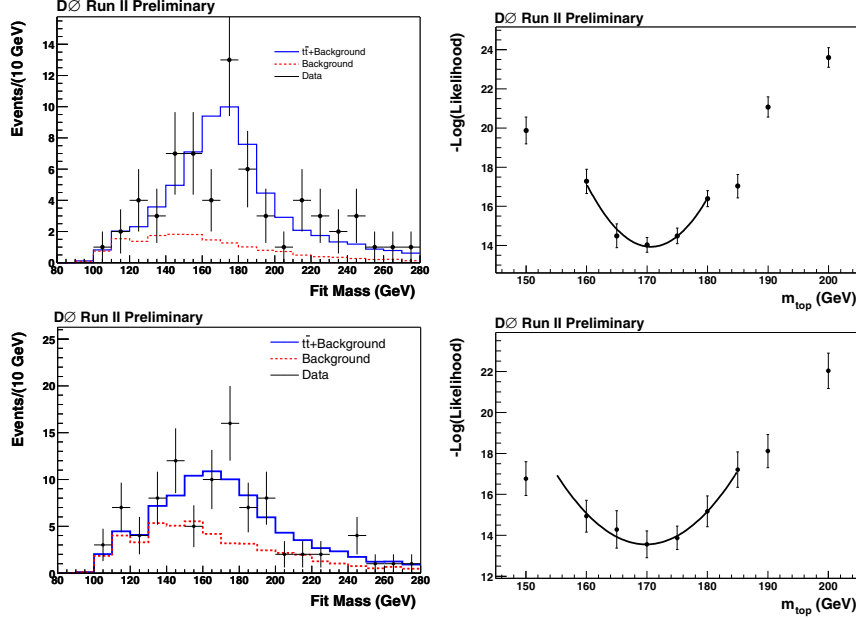


Figure 5: The result from the binned likelihood fit for the b -tagged (topological) analysis is presented on the upper (lower) left plot. The dots represent the data, the solid line is the fitted $t\bar{t}$ plus background and the dashed line is background only, normalized to the fraction returned by the fit. The right plots show the $-\ln(\mathcal{L})$ curves.

Two or more central jets with $E_T > 15$ GeV are required. A loose criterion is applied to the second lepton - it must have opposite charge but isolation is not mandatory. For the missing transverse energy the cut is increased to $\cancel{E}_T > 25$ GeV since two neutrinos are supposed to be presented in the event. If $\cancel{E}_T < 50$ GeV, a requirement for the angle between \cancel{E}_T and the nearest lepton or jet to be $\Delta\phi > 20^\circ$ is imposed. Also the transverse energy sum, H_T , has to be more than 200 GeV. Events due to cosmic rays, conversions or Z bosons are rejected.

Four major backgrounds are taken into account: di-boson plus jet production, W plus jets where one of the jet is faking a lepton, and Drell-Yan production, specially $Z/\gamma \rightarrow \tau\tau$. 33 events passed all cuts with an expected background of 11.6 ± 2.1 events.

In contrast to the lepton plus jets mode, in the dilepton case due to the presence of two neutrinos the kinematics is not constrained. The number

of non-measured kinematical variables is larger by one than the number of kinematic constraints ($-1CF$). Obviously, it is impossible to single out only one solution per event. We may take some event parameter (\vec{R}) as known in order to constrain the kinematics and then vary \vec{R} to determine a set of solutions. In order to determine a preferred mass, every solution should have a weight attached to it.

The minimal requirement in the case of $-1CF$ kinematics is to use a two dimensional vector as \vec{R} . We chose the azimuthal angles of the two neutrino momenta $\vec{R} = (\phi_{\nu 1}, \phi_{\nu 2})$ and create a net of solutions in the $(\phi_{\nu 1}, \phi_{\nu 2})$ plane.

For every point of the $(\phi_{\nu 1}, \phi_{\nu 2})$ plane we have 8 solutions. Two of them are generated by the two possibilities of associating the two charged leptons to the two leading jets which are assumed to originate from the $b\bar{b}$ partons. The four other solutions are generated from the four ways of associating each neutrino to two p_z momenta, satisfying the W decay kinematics. We select the minimal χ^2 solution for every point of the net for further use in our analysis.

Using the χ^2 value from a minimization we weight the selected solutions by $e(-\frac{\chi^2}{2})$. This is done in order to suppress the solutions which have worse compliance with the fit hypothesis.

The final extraction of the top quark mass from a sample of dilepton candidates is provided by the unbinned likelihood fit. The expected signal and background p.d.fs are obtained using Monte Carlo samples with detector simulation. The background-constrained fit ($N_b=11.6\pm 2.1$) returns: $M_{top} = 169.8 \pm_{9.3}^{9.2}$ GeV/c², with $23.4 \pm_{5.7}^{6.3}$ signal events. The left plot in Fig. 6 shows the fitted mass distribution. The insert shows the mass dependence of the negative log-likelihood function. The right plot represents the error distribution for Monte-Carlo simulated experiments, where the arrows indicate the data result.

We also performed a fit without constraining the number of background events. This fit returns $M_{top} = 169.2 \pm_{6.5}^{6.4}$ GeV/c², with $33.0 \pm_{5.8}^{6.0}$ signal events and $0.0 \pm_{0.0}^{4.2}$ background events.

4.2 D \bar{O} result

To reconstruct the top quark mass in the dilepton channel, D \bar{O} follows the ideas proposed by Dalitz and Goldstein in ¹⁷⁾. The analysis uses about 230 pb⁻¹ of data. The initial selection includes:

- two leptons, electron or muon, with $p_T > 15$ GeV in the pseudorapidity regions $|\eta(e)| < 1.1$ or $1.5 < |\eta(e)| < 2.5$ for the electron and $|\eta(\mu)| < 2.0$ for the muon. In e- μ events a separation cut of $\sqrt{\Delta\phi^2 + \Delta\eta^2} > 0.25$ is applied;
- two or more jets with $p_T > 20$ GeV in the pseudorapidity region $|\eta^{jet}| < 2.5$;

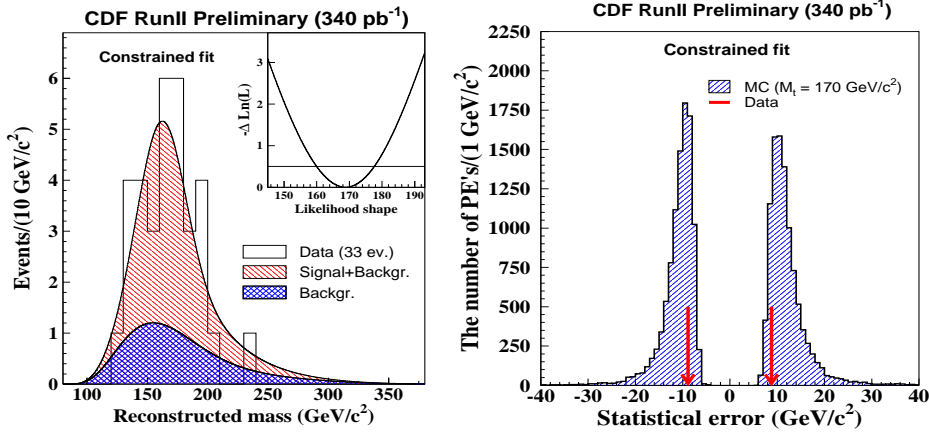


Figure 6: *Left: two-component constrained fit to the dilepton sample. The cross hatched area corresponds to the background returned by the fit and the line-shaded area is the sum of background and signal. The insert shows the mass-dependent negative log-likelihood used in the fit. Right: positive and negative error distributions returned by the fit in pseudo experiments. The arrows indicate the errors from the data fit.*

- large missing $\cancel{E}_T > 25$ GeV. However the \cancel{E}_T cut is varied for di-electron or di-muon events depending on the ee or $\mu\mu$ invariant mass;
- veto on the $Z \rightarrow ee, \mu\mu$ events;
- a cut $\Delta\phi(\mu, \cancel{E}_T) > 0.25$ rejects the events where the \cancel{E}_T and μ vectors are close to each other in the transverse plane;
- $H_T > 140$ GeV, where H_T is the scalar transverse momentum sum of the larger of the two lepton p_T s and of all jets over 15 GeV.
- for ee events a additional sphericity > 0.15 cut is applied.

8 $e\mu$, 5 ee and 0 $\mu\mu$ events satisfy all requirements, when 6.2 ± 0.6 , 2.8 ± 0.3 and 2.9 ± 0.6 events are correspondingly expected.

The $D\bar{O}$ analysis method can be summarized as follows. The momenta of the two highest p_T jets in the event are assigned to the $b\bar{b}$ from the decay of $t\bar{t}$ quarks. Then a likelihood to hypothesized values of the top mass in the region of $80\sim 280$ GeV is determined. For each event a solution is found when the pairs of $t\bar{t}$ momenta are consistent with the observed lepton and jet momenta and \cancel{E}_T . A weight to each solution is assigned as

$$\mathcal{W} = f(x)f(\bar{x})p(E_\ell^*|M_{top})p(E_{\bar{\ell}}^*|M_{top}), \quad (2)$$

where $f(x)$ ($f(\bar{x})$) is the parton distribution function for the proton (anti-proton) and the initial quark (anti-quark) is carrying a momentum fraction x (\bar{x}). $p(E_\ell^*|M_{top})$ denotes the probability for the top (anti-top) quark with a mass M_t to generate a lepton ℓ ($\bar{\ell}$) with the observed energy in the top quark rest frame.

There are two ways to assign the two jets to the b and \bar{b} quarks. In addition, for each jet-to-parton assignment, there might be up to four solutions for each hypothesized value of the mass, coming from the fact that every neutrino may have up to two real solutions for its p_z , satisfying the kinematics. Then the likelihood for each value of the top quark mass M_{top} is given by the sum of the weights $w_{i,j}$ over all possible solutions:

$$\mathcal{W}(M_t) = \sum_{p_z^\nu \text{ solutions}} \sum_{jet \text{ assignment}} w_{i,j}. \quad (3)$$

Up to now there was an implicit assumption that all momenta are measured perfectly. Therefore the weight in (3) is zero if no exact solutions are found. To account for detector resolution the weight calculations are repeated with input values for the particle momenta drawn from Gaussian distributions with means equal of the measured values and widths corresponding to the detector resolution. In addition the \cancel{E}_T value is recalculated from generated particle momenta and a random noise from a normal distribution with mean 0 GeV and rms 8 GeV is added. Figure 7 up (down) shows the weight curves for $e\mu$ (ee) events before (solid line) and after (shadow area) resolution smearing. For each event the value of the top quark mass at which the weight curve reaches its maximum is used as the estimator of the mass. After that, to extract the most probable top mass value from the data sample, a standard template method which exploits a binned maximum likelihood fit is applied. The likelihood fit returns $M_{top} = 155.{}^{+14}_{-13}(stat.) \pm 7.(syst.)$ GeV/ c^2 . The JES uncertainty (5.6 GeV/ c^2) dominates the systematic error.

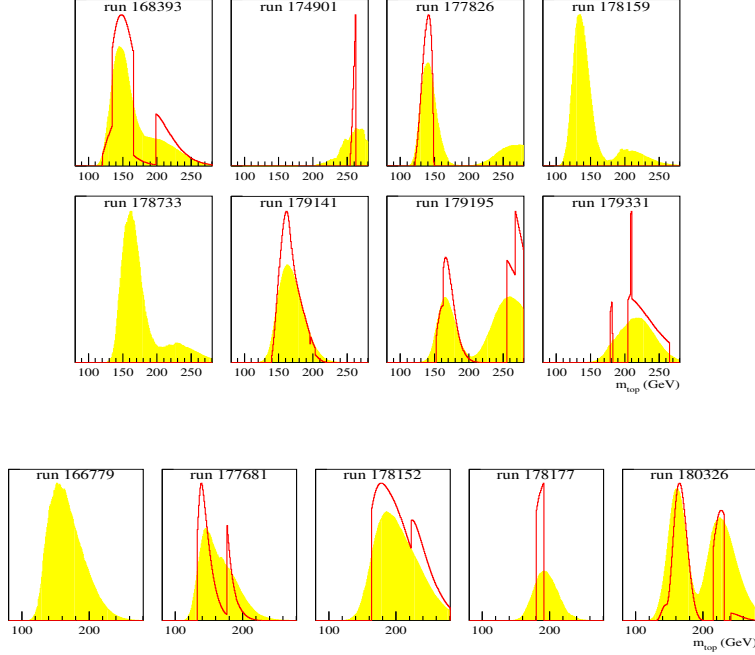


Figure 7: *Weight curves from 8 ep events (top) and 5 ee events (bottom). The shadow histograms show the weight curves with resolution smearing while the open histograms represent the weight curves without resolution smearing.*

5 Summary of the Top Quark Mass Measurements and Run II Prospects

Combining the presently available most accurate Run II CDF and DØ measurements in the dilepton and lepton plus jets decay topologies, one finds $172.7 \pm 3.5 \text{ GeV}/c^2$. This result is unofficial. The average is made by the author assuming simple correlations (0 or 1) between the systematic uncertainties in the CDF and DØ measurements.

The expected CDF uncertainty for JES systematics as a function of integrated luminosity is shown in Figure 8, left. The right plots shows the total top mass error versus integrated luminosity for the CDF lepton plus jet analysis. One may conclude that with a Run II integrated luminosity of 8 fb^{-1} the top quark mass could be measured by CDF with a precision of $\sim 2.0 \text{ GeV}/c^2$. This optimistic forecast is based on the present understanding that both the statisti-

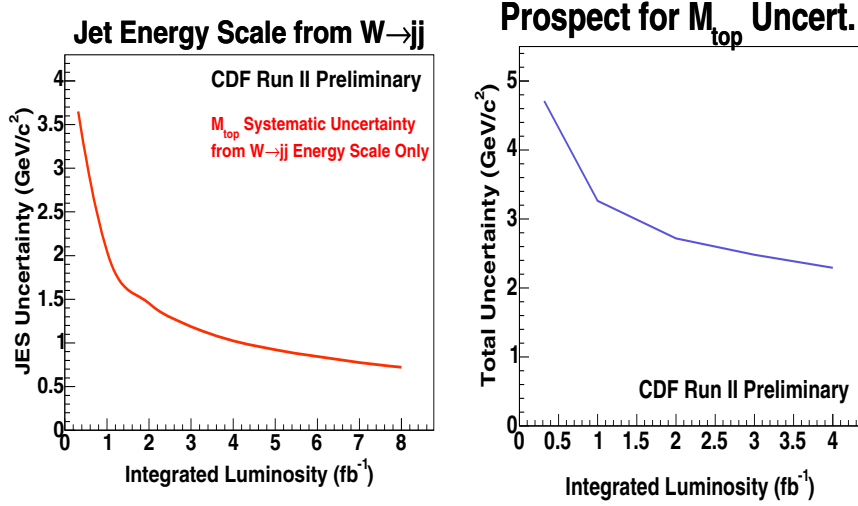


Figure 8: The expected JES uncertainty from $W \rightarrow jj$ as a function of integrated luminosity is shown on the left plot. On the right, the total expected top mass uncertainty, from CDF lepton plus jets events as a function of integrated luminosity, is shown.

cal and JES systematic uncertainties will decrease as expected with increasing integrated luminosity.

6 Conclusion

The top quark CDF results from the Tevatron 2002-2004 Run II, with an integrated luminosity of 318 and 230 pb^{-1} for CDF and DØ are presented. The best, up to date, measurement of the top quark mass from the CDF lepton plus jets analysis is $173.5^{+3.9}_{-3.8} \text{ GeV}/c^2$. Combining the CDF and DØ dilepton and lepton plus jets Run II results, the author's average of the top quark mass is $172.7 \pm 3.5 \text{ GeV}/c^2$.

7 Acknowledgments

I would like to thank the organizers for their invitation and hospitality. This work is supported by the U.S. department of Energy and CDF and D O collaborating institutions and their funding agencies.

References

1. F. Abe *et al.*, Phys. Rev. D **50**, 2966 (1994) and Phys. Rev. Lett. **73**, 225 (1994).
2. F. Abe *et al.*, Phys. Rev. Lett. **74**, 2626 (1995).
3. S. Abachi *et al.*, Phys. Rev. Lett **74**, 2632 (1995).
4. C. Parkes, "W Boson Properties at LEP", these proceedings.
5. F. Fielder, "Top Properties and Cross Section", these proceedings.
6. B. W. Harris, E. Laenen, L. Phaf, Z. Sullivan, S. Weinzierl Phys. Rev. D **66**, 054024 (2002).
7. C. Quigg, **FERMILAB-Pub-97/091-T**.
8. D. Acosta *et al.*, hep-ex/0410041, (2004).
9. D. Kestenbaum, Ph.D. Thesis (unpublished), Harvard University (1996).
10. T. Affolder *et al.*, Phys. Rev. D **63**, 03203 (2001).
11. B. Abbott *et al.*, Phys. Rev. Lett **58**, 052001 (1998).
12. R. H. Dlaitz and G. R. Goldstein, Proc. R. Soc. London A **445**, 2803 (1999).
13. K. Kondo, J. Phys. Soc. **57**, 4126 (1998).
14. V. M. Abazov *et al.*, Nature **429**, 638 (2004).
15. DØ Public note *et al.*, <http://www-d0.fnal.gov/Run2Physics/WWW/results/top.htm>.
16. D. Acosta *et al.*, Phys. Rev. Lett. **94**, 091803 (2005).
17. R. H. Dlaitz and G. R. Goldstein, Phys. Rev. D **45**, 1531 (1992).